

Regulation on BCAAs catabolism pathway plays the key role in cyclophosphamide-induced leucopenia BALB/c mice after the treatment of a typical Traditional Chinese Medicine of Lvjiao Buxue Granules

Jun-sheng Tian (✉ mikal2008@sina.com)

Shanxi University

Hui-liang Zhao

Shanxi University

Qi Wang

Shanxi University

Huan Xiang

Shanxi University

Xiang-ping Xu

Jiuzhitang Co.Ltd.Hunan

Sheng Huang

Jiuzhitang Co.Ltd.Hunan

Dong-lan Yan

Jiuzhitang Co.Ltd.Hunan

Xue-mei Qin

Shanxi University

Research

Keywords: Lvjiao Buxue Granules, leucopenia, metabolomics, nuclear magnetic resonance, biological targets network

Posted Date: June 2nd, 2020

DOI: <https://doi.org/10.21203/rs.3.rs-31132/v1>

License:   This work is licensed under a Creative Commons Attribution 4.0 International License.

[Read Full License](#)

Abstract

Background: Cyclophosphamide is a common tumor chemotherapy drug used to treat various cancers, but the resulting immunosuppression leads to leukopenia, which is a serious limiting factor in clinical application. Therefore, the introduction of immunomodulators as adjuvant therapy may help to reduce the hematological side effects of cyclophosphamide. Lvjiao Buxue Granules has been widely used in clinical treatment of gynecological diseases such as anemia and irregular menstruation, and recently, it has been found to increase the role of white blood cells, but its mechanism of action is still unclear. In this research, we applied the $^1\text{H-NMR}$ metabolomics approach to characterize metabolites in cyclophosphamide-induced leukopenia mice spleen, so as to fully understand the metabolic processes of leukopenia and improve the leukocyte function of Lvjiao Buxue Granules.

Methods: Cyclophosphamide was used to establish the leukopenia mice with cancer chemotherapy and the content of white blood cells, red blood cells, hemoglobin, platelets, and other routine blood indexes were measured. The changes of endogenous metabolites in spleen analyzed by $^1\text{H-NMR}$ metabolomics technique were investigated the regulation effect of LBG in mice with leukopenia. Afterward, the chemical components-targets-differential metabolites network of Lvjiao Buxue Granules was constructed by the use of biological targets network, thus leukopenia-relevant metabolism pathways were dissected.

Results: The blood routine parameters and organ indexes levels of leukopenia mice with cancer chemotherapy were improved by Lvjiao Buxue Granules. The metabolomic study revealed that 15 endogenous metabolites in mice spleen were considered as potential biomarkers of Lvjiao Buxue Granules for its protective effect. Integrated analysis of metabolomics and biological targets network indicated that Lvjiao Buxue Granules exerted the leukocyte elevation activity by inhibiting the branched-chain amino acids (BCAAs) degradation pathway and increasing the levels of valine, leucine and isoleucine.

Conclusion: Lvjiao Buxue Granules exert obvious efficacy on the mice model of leukopenia, which could be improved by regulating the branched-chain amino acid degradation pathway and the levels of valine, leucine and isoleucine.

Background

Cyclophosphamide is the most common cancer chemotherapy agent and used in anticancer for various types of cancer, especially breast cancer [1, 2]. Unfortunately, immunosuppression induced by cyclophosphamide causes the occurrence of leukopenia, which is a seriously limiting factor in clinical application [3, 4]. Therefore, introducing immunomodulatory agents as supportive therapy might be useful in alleviating hematotoxicity side effects of cyclophosphamide.

After constant efforts, the treatment against side effects of chemotherapy still leaves much to be desired. In recent years, Prescriptions made from a combination of multiple drugs have been considered as a promising therapeutic strategy for improving anti-tumor effects and reducing the side effects of

chemotherapy drugs [5]. Traditional Chinese medicine (TCM) prescriptions are usually made up of some different kinds of herbs, with the advantages of low toxicity and multiple targets [6]. Through overall and multi-target therapies, it has a comprehensive therapeutic effect in multi-factorial diseases.

In the past few decades, as good medicine for deficiency of Qi and blood, fatigue and weakness, Lvjiao Buxue Granules has been widely used in the clinical treatment of anemia irregular menstruation and other gynecological diseases, and recently it has been discovered elevating leukocytes effect [7]. However, the research on drug efficacy and mechanism of action is relatively rare. Lvjiao Buxue Granules generally comprised of 6 herbs: *Asini Corii Colla*, *Astragali Radix*, *Codonopsis Radix*, *Rehmanniae Radix Praeparata*, *Atractylodis Macrocephalae Rhizoma* and *Angelicae Sinensis Radix* at a ratio of 36:30:30:20:15:10.

Specific immune function can be stimulated by *Asini Corii Colla* in cyclophosphamide-induced mice [8]. The compatibility of *Astragali Radix* and *Angelicae Sinensis Radix* (Such as Danggui Buxue Tang is the famous prescription and is formed of *Astragali Radix* and *Angelicae Sinensis Radix*.) could increase the quantity of bone marrow mononuclear cells and peripheral blood leukocyte, enhance immunity and improve microcirculation [9]. Some other previous studies have also demonstrated that *Codonopsis Radix*, *Rehmanniae Radix Praeparata* and *Atractylodis Macrocephalae Rhizoma* exhibited effects of leukocyte elevation and Immuno-enhancement [10, 11]. Moreover, all the above herbs in the Lvjiao Buxue Granules are commonly and safely used in the formula of TCM, and rare adverse reactions were reported in clinical applications. However, up to now, the action mechanism of Lvjiao Buxue Granules in the treatment of leucopenia remained poorly understood.

In recent years, metabolomics is used to clarify the scientific effects related to the effectiveness mechanism, material basis and compatibility of TCM, and it will provide the technical support for the evaluation of the effectiveness of TCM, the basis of prescription substances and the understanding essence of TCM syndromes [12-14]. With the continuous development of metabolomics technology, it has been increasingly concentrated on metabolomics to reveal the pharmacodynamics and mechanisms of TCM prescriptions, such as Xiao Yao San and Baihe Dihuang Tang [15, 16]. In this research, we applied the ¹H-NMR metabolomics approach to characterize metabolites in cyclophosphamide-induced leucopenia mice spleen, so as to fully understand the metabolic processes of leucopenia and improve the leukocyte function of Lvjiao Buxue Granules.

In this study, we firstly constructed a leucopenia mice model with cancer chemotherapy, in which mice manifest similar syndromes to those of patients with leucopenia in the clinic. We then tested metabolites in mice spleen and compared the levels of endogenous metabolites between healthy mice, leucopenia mice and leucopenia mice treated with Lvjiao Buxue Granules, and revealed the related metabolic pathways as well. Next, this study was applied to Biological targets network analysis methods to generate a leucopenia “chemical components-targets-differential metabolites” regulatory network centered. Finally, through a comprehensive analysis of the biological target network and metabolomics results, a regulatory network for the “herb-chemical-constituent-targets-pathway- metabolites” was constructed to characterize the pharmacological effect of Lvjiao Buxue Granules in the treatment of

leukopenia. The strategies on characterizing the main constituents of Lvjiao Buxue Granules and its therapeutic effects and mechanisms of leukopenia will provide a theoretical basis for the clinical application of this traditional Chinese medicine prescription.

Materials And Methods

Materials

Cyclophosphamide was obtained from Jiangsu Shengdi Pharmaceutical Co., Ltd (Batch No. 18051125, Jiangsu, China). D₂O was purchased from Norell (Landisville, USA). K₂HPO₄·3H₂O and NaH₂PO₄·2H₂O were obtained from Wuhan Yuancheng Technology Development Co., Ltd. (Wuhan, China). Lvjiao Buxue Granules was purchased from Jiuzhitang Co., Ltd. (Batch No. 201802029, Hunan, China), which production method conforms to the standard of Chinese Pharmacopoeia (2015 edition). Diyu Shengbai tablets were obtained from Chengdu Diao Co., Ltd. (Batch No. Z20026497, Chengdu, China). The enzyme-linked immunosorbent assay (ELISA) kits were obtained from MEIMIAN (Jiangsu, China).

Animals

Inbred strain female (6-8 weeks old) BALB/c mice, weighing 18-20 g, provided by Vital River Laboratory Animal Technology Co., Ltd. (Beijing) (License number SCXK-2016-0006). The animals were kept at room temperature (24±1) °C, humidity (60±5)%, and freely eating under the natural rhythm of day and night before the experiments. All animal experiments were conducted in accordance with the NIH Guidelines for Care and Use of Laboratory Animals (U.S.A) and the Prevention of Cruelty to Animals Act (1986) of China, and these experiments were also approved by the Animal Ethics Committee of Shanxi University.

Development of leukopenia mice model and treatment protocols

Animals were randomly divided into a normal control group and five cyclophosphamide induced groups: control group (C), model group (M), low dose of Lvjiao Buxue Granules group (LBG-L), moderate dose of Lvjiao Buxue Granules group (LBG-M), high dose of Lvjiao Buxue Granules group (LBG-H), and Diyu Shengbai tablets group (DST), each group was consists of 8 mouse. The mice in LBG-L, LBG-M, or LBG-H groups were administered Lvjiao Buxue Granules (3 g/kg, 6 g/kg, 12 g/kg) suspension daily, and the mice in the DST group were administered Diyu Shengbai tablets (0.14 g/kg) suspension daily. Mice in the control and model groups received an equal volume of vehicle orally. The 4T1 breast cancer model was established in which the tumor grew to approximately 5*5 cm². The five cyclophosphamide-induced groups would be injected with cyclophosphamide in the dose of 80 mg/kg by intraperitoneal to 4T1 breast cancer model on the 1st day, 3rd day, 5th day and 7th day individually. The treatment lasted for 7 days, and the state of the mice was observed and the weight was measured daily.

Sample collection and determination

After 1h of the last treatment on the 7th day, 0.4 mL blood samples were collected into 1.0 mL tube with EDTA within via the orbital blood. Animal blood analyzer (HEMAVET950) was applied to evaluate peripheral blood routine parameters of 400 μ L whole blood: white blood cell count (WBC), neutrophil count (NE), lymphocyte count (LY), monocytes count (MO), red blood cell count (RBC), hemoglobin (HGB), red blood cell volume (HCT), platelet count (PLT), mean red cell volume (MCV) and mean corpuscular hemoglobin (MCH). On the 8th day, mice were sacrificed, and spleen, thymus and liver tissues were immediately weighed and collected. The calculation formula of the organ index is as follows: organ index = organ weight (mg)/bodyweight (g). Quickly transfer the spleen to a refrigerator at -80 °C and use it for metabolomics analysis.

Sample preparation for NMR measurements

After thawing the spleen tissue, take about 40 mg, cut it (on ice), add 650 μ L of MeOH and H₂O (v/v, 2:1) to a 2 mL centrifuge tube, and homogenize and extract twice on an ice bath. The homogenate was centrifuged at 4 °C, 13 000 r·min⁻¹ for 15 min. The supernatants were combined, transferred to a 2 mL centrifuge tube and blown with nitrogen. The dried sample was dissolved in 700 μ L of phosphate buffer (pH 7.40, containing D₂O, 0.1 mo/L, Na₂HPO₄/Na H₂PO₄, 0.01% TSP), centrifuge at 13 °C, 13,000 r·min⁻¹ for 20 min, 600 μ L supernatant was transferred into a 5 mm NMR tube for ¹H NMR analysis.

Metabolomics analysis

The ¹H NMR spectral data were collected on a Bruker 600 MHz AVANCE III NMR spectrometer (Bruker, Germany). The sample was the Noesygppr1d sequence to suppress the water peak. The number of scans was 64 scans, and each scan required an acquisition time of 2.654s. The specific parameters were as follows: spectral width was 12 345.7 Hz; spectrum size was 65 536 data points; pulse width (PW) was 30° (12.7 μ s); fourier transform LB was 0.3 Hz and relaxation delay time was 1.0 s. The ¹H NMR spectrum of the spleen was corrected for chemical shifts using TSP (δ 0.00) as the standard. The spectrum in the region of δ 0.60 to 9.49 was divided into 0.01 equal widths and integrated. All resulting integration data are “mass” normalized to eliminate weight differences of spleen tissue.

Simca-P 14.1 (Umetrics, Sweden) was used to perform multivariate data analysis. Firstly, by principal component analysis (PCA) of the normalized data, to identify the degree of dispersion between the control group and the model group, and the outliers were eliminated. Next, partial least-squares discriminant analysis (PLS-DA) was used to distinguish the differences in metabolic profiles between the control, model and drug groups. Orthogonal-projection to latent structure-discriminant analysis (OPLS-DA) was used to find differential metabolites between the control group and the model group. Finally,

ANOVA analysis was performed on the metabolites in SPSS 16.0 software, with $P < 0.05$ as differential metabolites.

Biological targets network analysis

All components of Lvjiao Buxue Granules were collected from the TCMSP database. For all ingredients, the initial structure formats (e.g., mol2 and SDF) were transformed into a unified SDF format using the Open Babel toolkit (version 2.4.1). The ingredients with suitable $OB \geq 30\%$ and $DL \geq 0.18$ were chosen as candidate ingredients for further research, which is used as a selection criterion for the ingredients in the traditional Chinese herbs. After ADME screening, some ingredients that did not meet the three screening criteria were also selected because of their high content and high biological activity. All databases and software mentioned above are public.

The PharmMapper server was used for potential target prediction analysis. Metabolite data were imported in Metascape, a plugin of Cytoscape 3.7.1 and subjected to metabolic enzyme analysis. Finally, Cytoscape 3.7.1 software was used to construct the “herb-chemical constituent-targets-pathway-metabolite” regulatory network of Lvjiao Buxue Granules for leucopenia treatment.

Determination of the levels of BCKDHA and ACADS

In order to further verify the results of biological targets network, the content of the key rate-limiting enzymes BCKDHA (branched chain keto acid dehydrogenase E1, alpha polypeptide) and ACADS (Acyl-CoA Dehydrogenase Short Chain) on the BCAAs degradation pathway were determined. The levels of BCAAs and the degradation rate of them could be affected by the content of these enzymes.

The levels of BCKDHA and ACADS in the liver tissue lysates were determined by ELISA kits according to manufacturer instructions.

Results

Effect of LBG on blood routine parameters and organ indexes in cyclophosphamide-treated mice

The biochemical indexes of the peripheral blood were observed by evaluating the blood toxicity of cyclophosphamide. The parameters of WBC, NE, LY, MO, RBC, HGB, HCT and MCH in the model group were significantly lower than those in the control group ($P < 0.01$; Table 1), and the PLT parameters were significantly higher than those of the control group ($P < 0.05$; Table 1). The increase and decrease of these peripheral blood routine parameters are the main diagnostic criteria of leukopenia, indicating that the model of leukopenia was successfully replicated. Compared to the model group, the expressions of WBC, NE, LY, MO, RBC, HGB and MCH in the LBG-L, LBG-M and LBG-H were significantly increased ($P < 0.05$;

Table 1), and the efficacy was better than the DST group. The results suggested that Lvjiao Buxue Granules exerted well effect on leukocyte elevation activity.

Table 1
Changes in indexes of blood routine examination on leucopenia mice with LBG treatment (n = 8)

Groups	WBC (10 ⁹ /L)	NE (10 ⁹ /L)	LY (10 ⁹ /L)	MO (10 ⁹ /L)	RBC (10 ¹² /L)
C	4.63±0.58	0.52±0.11	3.61±0.42	0.18±0.04	9.99±0.43
M	1.83±0.25 ^{##}	0.25±0.04 ^{##}	1.45±0.21 ^{##}	0.13±0.04 [#]	8.01±0.23 ^{##}
LBG-L	3.03±0.44 ^{**}	0.54±0.12 ^{**}	2.24±0.35 ^{**}	0.25±0.04 ^{**}	8.69±0.18 ^{**}
LBG-M	3.33±0.48 ^{**}	0.55±0.14 ^{**}	2.41±0.38 ^{**}	0.36±0.10 ^{**}	8.63±0.12 ^{**}
LBG-H	2.60±0.20 ^{**}	0.41±0.16 [*]	1.88±0.12 ^{**}	0.31±0.09 ^{**}	8.44±0.18 ^{**}
DST	2.79±0.36 ^{**}	0.36±0.14 [*]	2.08±0.31 ^{**}	0.30±0.09 ^{**}	8.00±0.29
Groups	HGB (g/L)	HCT (%)	PLT (10 ⁹ /L)	MCV (fl)	MCH (pg)
C	149.50±2.78	58.69±1.36	539.13±54.19	58.66±0.64	15.56±0.37
M	124.50±2.56 ^{##}	49.50±2.32 ^{##}	615.75±52.30 [#]	58.89±0.40	14.28±0.15 ^{##}
LBG-L	135.00±5.93 ^{**}	52.11±2.08 [*]	605.63±40.60	59.08±0.48	15.59±0.24 ^{**}
LBG-M	132.75±1.04 ^{**}	51.39±1.03	602.25±22.28	59.35±0.61	15.69±0.24 ^{**}
LBG-H	130.25±2.82 ^{**}	49.1±1.59	622.13±47.92	59.68±0.53	15.79±0.14 ^{**}
DST	128.88±5.06	50.09±2.25	612.38±58.24	60.16±0.59	15.60±0.33 ^{**}
Data are expressed as mean ± S.D. of eight mice. WBC: white blood cell count; NE: neutrophil count; LY: lymphocyte count; MO: monocytes count; RBC: red blood cell count; HGB: hemoglobin; HCT: red blood cell volume; PLT: platelet count; MCV: mean red cell volume; MCH: mean corpuscular hemoglobin.					
# <i>P</i> < 0.05 vs. C group; ## <i>P</i> < 0.01 vs. C group					
* <i>P</i> < 0.05 vs. M group; ** <i>P</i> < 0.01 vs. M group					

Compared to the control group, the mice in the model group had an enlargement of the liver ($P \leq 0.05$; Fig. 1C), and reduction of the spleen ($P \leq 0.01$; Fig. 1A) and thymus ($P \leq 0.01$; Fig. 1B). The administration of LBG and DST over 7 days reversed the viscera lesions of mice with hematopoietic dysfunction ($P \leq 0.05$; Fig. 1).

NMR metabolomics analysis and multivariate data analysis

Analysis of ^1H -NMR spectrum of spleen tissue

Representative ^1H NMR spectra of metabolites for spleen tissue extracts from control group, model group and LBG-M group were displayed in Fig. 2. Specific metabolites in spleen tissue extracts were identified through literature and NMR databases (HMDB (<http://www.hmdb.ca/>) and BMBB (<http://www.bmrb.wisc.edu/>)) Further confirmed. In total, 32 metabolites were identified, belonging to amino acids, organic acids, sugars, lipids, etc. The details of metabolites were listed in Table 2.

Table 2

¹H NMR assignments of major metabolites from mice spleen tissues

No.	Metabolites	Components assignment	Chemical shift (δ ¹ H ppm)
1	Isoleucine	δ -CH ₃ , γ -CH ₃ , γ -CH ₂ , γ -CH ₂ ', β -CH, α -CH	0.94(t), 1.01(d), 1.27(m), 1.47(m), 1.98(m), 3.68(d)
2	Leucine	δ -CH ₃ , δ' -CH ₃ , β -CH ₂ , γ -CH, β -CH ₂ ', α -CH	0.96(d), 0.97(d), 1.70(m), 1.72(m), 1.74(m), 3.74(m)
3	Valine	γ -CH ₃ , γ' -CH ₃ , β -CH, α -CH	0.99(d), 1.05(d), 2.28(m), 3.62(d)
4	3-hydroxybutyrate	γ -CH ₃ , α -CH ₂ , α -CH ₂ ', β -CH	1.20(d), 2.31(dd), 2.41(dd), 4.16(m)
5	Lactate	β -CH ₃ , α -CH	1.33(d), 4.11(q)
6	Alanine	β -CH ₃ , α -CH	1.48(d), 3.78(d)
7	Lysine	γ -CH ₂ , γ -CH ₂ ', δ -CH ₂ , β -CH ₂ , ϵ -CH ₂ , CH	1.45(m), 1.51(m), 1.73(m), 1.91(m), 3.03(t), 3.76(t)
8	Glutamate	β -CH ₂ , β -CH ₂ ', γ -CH ₂ , CH	2.07(m), 2.13(m), 2.35(m), 3.76(dd)
9	Methionine	δ -CH ₃ , β -CH ₂ , γ -CH ₂ , α -CH	2.13(s), 2.14(m), 2.64(t), 3.85(m)
10	Glutamine	β -CH ₂ , γ -CH ₂ , CH	2.14(m), 2.46(m), 3.78(t)
11	Pyruvate	CH ₃	2.37(s)
12	Aspartate	CH ₂ , CH ₂ ', CH	2.68(dd), 2.82(dd), 3.90(dd)
13	Acetate	CH ₃	1.93(s)
14	Creatine	CH ₃ , CH ₂	3.04(s), 3.94(s)
15	Myo-inositol	2-CH, 4/6-CH, 1/3-CH, 5-CH	3.29(t), 3.54(dd), 3.63(dd), 4.07(t)
16	Choline	(CH ₃) ₃ , N-CH ₂ , OH-CH ₂	3.21(s), 3.52(m), 4.07(m)
17	Phosphocholine (PC)	CH ₃ , N-CH ₂ , O-CH ₂	3.22(s), 3.59(m), 4.18(m)
18	Glycerophosphocholine (GPC)	CH ₃ , OH-CH ₂ , N-CH ₂ , OH-CH, NCH ₂ CH ₂	3.23(s), 3.68(m), 3.68(m), 3.92(m), 4.33(m)
19	Taurine	S-CH ₂ , N-CH ₂	3.28(t), 3.43(t)
20	Glycine		3.57(s)

		CH ₂	
21	α -glucose	4-CH, 2-CH, 3-CH, CH ₂ , CH ₂ ', 5-CH, 1-CH	3.41(m), 3.59(m), 3.73(m), 3.73(m), 3.85(m), 3.85(m), 5.26(d)
22	β -glucose	2-CH, 3/5-CH, CH ₂ , CH ₂ ', 1-CH	3.29(m), 3.52(m), 3.74(m), 3.91(dd), 4.66 (d)
23	Uracil	5-CH, 6-CH	5.81(d), 7.55(d)
24	Uridine	ribose-2-CH, uracil-C-CH, uracil-N-CH	5.90(d), 5.92(d), 7.88(d)
25	Cytidine	ribose-2-CH, ring-5-CH, ring-6-CH	5.92(d), 6.07(d), 7.85(d)
26	Fumarate	CH	6.51(s)
27	Tyrosine	CH ₂ , CH ₂ ', N-CH, 3/5-CH, 2/6-CH	3.06(dd), 3.19(dd), 3.94(dd), 6.90(m), 7.20(m)
28	Phenylalanine	CH ₂ , CH ₂ ', N-CH, <i>o</i> -CH, <i>p</i> -CH, <i>m</i> -CH	3.13(dd), 3.28(dd), 4.00(dd), 7.33(m), 7.38(m), 7.43(m)
29	Xanthine	CH	7.90(s)
30	Hypoxanthine	2-CH, 7-CH	8.20(s), 8.22(s)
31	Formate	HCOOH	8.46(s)
32	Trimethylamine-N-oxide(TMAO)	CH ₃	3.28(s)

LBG regulates metabolic disorders in leukopenia mice

To excavate the specific marker metabolites that resulted in differentially expressed metabolite changes in mice caused by cyclophosphamide-induced leukopenia, the supervised multivariate methods PLS-DA and OPLS-DA were used for processing. (Fig. 3). The PLS-DA pattern recognition analysis of all the group trends was shown in Fig. 3A, in which the control group was completely separated from the model group, and the LBG-L, LBG-M, LBG-H groups were separated from the model group, with a tendency closer to the control. It was indicated that the leukopenia model was successfully established and the Lvjiao Buxue Granules exhibited an excellent leukocyte elevation effect.

The validity of the analysis was performed by using 200 permutation tests, in which all R² and Q² values were lower than the original ones. (Intercepts: R²=0.854, Q²=0.649) (Fig. 3B). Furthermore, differential metabolites between control and the model groups were discovered by OPLS-DA, which is a supervised pattern recognition method that could improve the discovery effect of differential metabolites (Fig. 3C). The corresponding loading (S+V)-plot with color-coded was illustrated in Fig. 3D, and the metabolites

contributed to the leukocyte elevation effect were identified by corresponding (S+V)-plots and statistical analysis.

The disturbed metabolite variances of the different groups could be related to the metabolic changes associated with leucopenia and the increase of leukocytes in Lvjiao Buxue Granules. The changes of the differential metabolites between control and model groups in mice spleen were shown in Fig. 4. Compared with the control group, the elevated levels of TMAO, pyruvate, GPC, taurine and glutamate in the model group were evident in the spleen samples from. Additionally, lower levels of choline, myo-inositol, tyrosine, valine, iso-leucine, PC, α -glucose, leucine and phenylalanine in the spleen of the model group compared with the control group we observed. The changes in these endogenous metabolites are considered to be a direct result of the leucopenia resulting from DST. Meaningfully, the levels of metabolites were regulated by LBG treatment (Fig. 4), suggesting that LBG may play a leukocyte elevation effect by leveling off the divergences of the metabolites.

Correlation analysis of differential metabolites, blood routine parameters and organ indexes

The blood routine parameters and organ indexes are well-known for the evaluation of leucopenia. An analysis of the correlation between the blood routine parameters, organ indexes and differential metabolites can be used to screen for specific biomarkers. Pearson's correlation analysis method was used for the investigation of the relationship among the differential metabolites, blood routine parameters and organ indexes of all groups. The correlation map was shown in Fig. 5A, where the color reflects the correlation strength and sign, the WBC, RBC, HGB, HCT, NE, LY, MO and MCH presented negative correlations with glutamate, pyruvate, aspartate, GPC, taurine and positive correlations with valine, iso-leucine, leucine, choline, PC, myo-inositol, α -glucose, tyrosine and phenylalanine. Besides, the fluctuation of the spleen index showed correlations with differential metabolites ($P \leq 0.01$) (Fig. 5A). The correlation network of blood routine parameters, organ indexes and differential metabolites based on Pearson's was shown in Fig. 5B, which could be served as differential metabolites for assessing the leucopenia and the effect of LBG.

Establishment of “different metabolites-enzymes/genes” metabolic network

The metabolic networks involved in a slice of enzymes and genes were constructed by using the Netscape plug-in running on Cytoscape 3.7.1, that the internal correlation of the differential metabolites based on enzyme or gene levels could be better understood (Fig. 6). As a result, 154 candidate genes or enzymes related to differential metabolites were tentatively found out, and they will be served as targets for subsequent biological targets network analysis for the construction of targets-metabolites interactions network (Fig. 6). Finally, to map the metabolic pathway of identified differential metabolites

from leucopenia-associated researches, the enrichment analysis was performed and metabolic pathways were obtained for further investigation.

Biological targets network and metabolomics integration analysis

Screening active compounds of Lvjiao Buxue Granules

In the current study, two ADME-related models, including OB and DL, were employed to screen for active ingredients in Lvjiao Buxue Granules. After ADME screening, some ingredients that did not meet the screening criteria were selected because of their high content and high biological activity. First of all, a gross of 87, 134, 76, 55 and 125 candidate ingredients were obtained from Astragali Radix, Codonopsis Radix, Rehmanniae Radix Praeparata, Atractylodis Macrocephalae Rhizoma, Angelicae Sinensis Radix, respectively. The ingredients were retrieved from these ingredients via the ADME parameters and literature confirmation. Consequently, a total of 35 chemical ingredients of Lvjiao Buxue Granules were filtered out for further analysis (Table S1).

Construction of “chemical components-targets-differential metabolites” regulatory network and correlative Pathways

490 targets of the 35 components in Lvjiao Buxue Granules were predicted using the Pharm Mapper server, and 28 of them were closely related to differential metabolites of leukopenia with a total frequency of 496 (Table S2). Cytoscape software was used to establish the “Chemical Components-Targets-Differential Metabolites” regulatory network of Lvjiao Buxue Granules, which was an indication that the correlations of 35 compounds, 28 metabolite-associated target proteins, and 11 differential metabolites were presented in Fig. 7. Analysis of the “Chemical Compositions-Targets” correlation revealed that multiple compounds could act on the same target, and multiple targets could be affected by the same compound. For instance, the L-amino-acid oxidase could be the target of ferulic acid, caffeic acid, biatractylolide simultaneously, while the compound of catalpol could act on Aldo-keto reductase family 1 member B1, Eukaryotic translation initiation factor 4E-binding protein 3, and Glucose-6-phosphatase at the same time (Fig. 7).

To assess the molecular mechanisms of Lvjiao Buxue Granules effects on leucopenia, the Cytoscape with its plugin ClueGO was utilized for KEGG pathway analysis, followed by the analysis of target-related pathway. A total of 9 significant pathways are predicted (in the term of P -Value \leq 0.05), among which the Valine, leucine and isoleucine degradation was the most closely related one (Table 3). According to the results of biological targets network and metabolomics, a preliminary prediction of the mechanism by which Lvjiao Buxue Granules plays leukocyte elevation activity could be as follows: Lvjiao Buxue

Granules can inhibit the Valine, leucine and isoleucine degradation and add the levels of Valine, leucine and isoleucine (Fig. 4A).

Table 3
The results of KEGG correlative pathways of LBG major active ingredient related targets analyzed by Cytoscape3.7.1 software

Rank	KEGG Term	P-Value	Associated Genes Found
1	Valine, leucine and isoleucine degradation	2.76E-10	ACAA1, ACAA2, BCAT1, BCAT2, DLD, HADHA, IL4I1
2	Glycolysis / Gluconeogenesis	3.46E-9	DLD, G6PC, GCK, HK1, LDHB, PKLR, PKM
3	Cysteine and methionine metabolism	1.06E-8	BCAT1, BCAT2, CTH, IL4I1, LDHB, SDS
4	Galactose metabolism	4.41E-6	AKR1B1, G6PC, GCK, HK1
5	Pyruvate metabolism	1.13E-5	DLD, LDHB, PKLR, PKM
6	Propanoate metabolism	2.10E-4	DLD, HADHA, LDHB
7	Starch and sucrose metabolism	2.99E-4	G6PC, GCK, HK1
8	Glycine, serine and threonine metabolism	4.10E-4	CTH, DLD, SDS
9	Fatty acid degradation	5.44E-4	ACAA1, ACAA2, HADHA

Molecular docking verification

The chemical-components-targets-differential metabolites regulatory network was constructed and the valine, leucine and isoleucine degradation pathway were focused that the correlations of 35 compounds, 7 metabolite-associated target proteins, and 3 differential metabolites were presented in Fig. S3. Furthermore, the Systems Dock (<http://systemsdock.unit.oist.jp/iddp/home/index>) method was used to evaluate the binding potential between selected Valine, leucine and isoleucine degradation pathway targets and the chemical components with top 7 degrees (Degree \geq 5) (Fig. S2). The docking score of SystemsDock can directly indicate the protein-ligand binding potential. The 3D structures and PDB ID of the above 7 selected targets were gathered from the PDB database (<https://www.rcsb.org/>) (Table S3). The results showed that 6 targets (ACAA2, BCAT1, BCAT2, DLD, HADHA and IL4I1) had 3D structures, while the 3D structure of ACAA1 did not exist. As shown in Fig. 8, the docking scores of 95 pairs of target-

compound combinations were mostly greater than native ligand, which showed that they possessed great binding activity.

Experimental validation of BCAAs catabolism pathway by ELISA

To further confirm the results of the biological targets network, we experiment to verify the BCAAs catabolism pathway. Two key and irreversible reactions of BCAAs catabolism require the participation of branched-chain keto acid dehydrogenase (BCKDH) complex and acyl-CoA dehydrogenase (ACAD). The levels of BCKDHA and ACADS were significantly increased ($P \leq 0.01$) in leukopenia model mice (Fig. 8). After oral administration of Lvjiao Buxue Granules, the levels of BCKDHA and ACADS were significantly reduced ($P \leq 0.05$ or $P \leq 0.01$). The BCKDHA and ACADS enzyme levels were significantly increased in the leukopenia model mice in the catabolism pathway of BCAAs. Abnormal expression of BCAAs degrading enzymes causes BCAAs overly decomposed in leukopenia model mice. Lvjiao Buxue Granules can reverse the levels of two enzymes, thereby improving the abnormal metabolism of BCAAs.

Discussion

In this study, we observed the efficacy profiles of low, intermediate and high dose Lvjiao Buxue Granules on the increase of leukocyte in mice with leukopenia caused by cancer chemotherapy for the first time. The major new findings were that in cyclophosphamide-induced leucopenia mice, treatment with Lvjiao Buxue Granules resulted in the following, accelerating recovery of spleen, thymus and liver indexes, accelerating recovery of WBC, NE, LY, MO and RBC content, and restoring the level of metabolites in the mice spleen caused by leukopenia. Thus, the in vivo treatment with Lvjiao Buxue Granules accelerates recovery of leukopenia mice. In this study, a comprehensive approach of metabolomics and biological targets network was performed to explore the biological mechanisms of Lvjiao Buxue Granules for treating leucopenia caused by cyclophosphamide-induced. According to the results of biological targets network and metabolomics, that regulation on the BCAAs catabolism pathway may play a key role in cyclophosphamide-induced leucopenia BALB/c mice after the treatment of a typical Traditional Chinese Medicine of Lvjiao Buxue Granules.

Leukopenia animal model

Cyclophosphamide, a cell cycle non-specific anti-tumor drug, is one of the most commonly used drugs for establishing an animal model of leukopenia [17, 18]. The cyclophosphamide can easily block the division and proliferation of normal hematopoietic cells, lead to impaired bone marrow regeneration or damage to the hematopoietic system, decrease the number of bone marrow nucleated cells, and decrease hematopoietic reconstitution activity. Among them, leukopenia is the most common result [19, 20]. By combing the literature, the cyclophosphamide-induced leukopenia model has been relatively mature, but the mouse species, dosage and duration are different, and it is mostly used to stimulate bone marrow suppression and immunosuppression caused by chemotherapy [4, 21-23]. However, in clinical practice,

the cyclophosphamide is used for chemotherapy in cancer patients, while animal models are often used in normal mice, which is different from clinical practice. In this research, the cyclophosphamide was given to establish a leukopenia model in cancer mice to simulate the clinical and pathological physiology.

Blood routine parameters

Hematopoietic dysfunction including leukopenia, hematopoietic suppression and immunosuppression were observed in patients receiving cyclophosphamide with malignant tumors. The occurrence of leukopenia may be related to hematopoietic stem cell dysfunction, apoptosis of bone marrow cells and imbalance of hematopoietic regulatory factors [24, 25]. Thus rebuilding hematopoietic function is the primary problem of adjuvant chemotherapy. In this work, significant decreases in WBC, NE, LY, MO, RBC and HGB were observed through the impact of cyclophosphamide, and these altered blood routine parameters were regulated by Lvjiao Buxue Granules treatment. The cyclophosphamide can degrade to amido nitrogen mustard, acrolein and so on, which bind to the DNA of rapidly growing cells and produce strong toxicity in the cells, while Lvjiao Buxue Granules may play a role of leukocyte elevation through the reduction of DNA damage and improvement of bone marrow hematopoietic function [26]. Cyclophosphamide can degrade aldehydes, phosphoramides, nitrogen mustard and acrolein.

Organ indexes

As the most important immune organs in mammals, spleen and thymus are the places where immune cells grow and proliferate [27]. The developmental status of the spleen and thymus directly affects immune function and disease resistance [28-30]. The results of this experiment showed that the spleen and thymus indexes of the high, medium and low dose Lvjiao Buxue Granules groups were significantly higher than those of the cyclophosphamide-induced group. It is suggested that Lvjiao Buxue Granules could resist the toxic effects of cyclophosphamide on the development of spleen and thymus. Since the cyclophosphamide is metabolized in the liver which is the tissue represents a major target for cyclophosphamide-induced tissue damage [31, 32]. The liver is the main drug metabolism organ in mammals. Metabolized cyclophosphamide causes damage to mitochondria and damage to cellular respiration, which affects the onset of lipid peroxidation and an increase in reactive oxygen species [33, 34]. In this work, significant increases in Liver index were observed through the impact of cyclophosphamide, and this altered were regulated by Lvjiao Buxue Granules' treatment. Hence, Lvjiao Buxue Granules plays a role in increases in the Liver index through reduced lipid peroxidation and reactive oxygen species production.

BCAAs catabolism

The branched-chain amino acids (BCAAs) catabolism have been focused on a great deal of diseases, especially liver cirrhosis, renal failure, sepsis and cancer (Fig. 9) [35]. Numerous studies have shown that

BCAAs have a positive effect on regulating body weight, muscle protein synthesis, insulin secretion, the aging process, and prolonging the healthy period [36-38]. BCAAs have been shown to an important role in regulating body metabolism and maintaining energy balance by directly affecting body tissues, such as white adipose tissue, liver tissue and muscle tissue [39]. BCAAs can be used as energy substrates in catabolic states, which can be directly oxidized or converted to gluconeogenic-cholesterogenic substrates in the muscle. In contrast, BCAAs stimulate protein synthesis and cell growth in anabolic conditions [40].

In the current study, we used 19 active ingredients of Lvjiao Buxue Granules as a probe to conduct molecular docking with potential targets of BCAAs catabolism, and the molecular docking showed that they possessed great binding activity. A study revealed that astragaloside Ⅳ, formononetin, calycosin and ferulic acid showed promoting hematopoiesis through regulating cyclin-related proteins, promoting cell cycle transformation, and promoting HSC proliferation [41]. Another study showed that caffeic acid can down-regulated the expression of TLR-2 and HLA-DR, and inhibited the production of cytokines, then exerted an immunomodulatory action on human monocytes [42]. Studies of receiver biases suggest that the chemical composition of the Lvjiao Buxue Granules has a better activity of immunity regulation and hematopoiesis. The results of molecular docking showed that there were complex interactions between them, which showed the characteristics of multi-components and multi-targets. In this study, the levels of valine, leucine and isoleucine decreased significantly in the cyclophosphamide-induced mice, which was a suggestion that the leukopenia was associated with the branched-chain amino acids catabolism. Moreover, the branched-chain amino acids were positively correlated with WBC, NE, LY and MO in the leucopenia mice, which were an indication that they played key roles in the progression of leucopenia. Compared with cyclophosphamide-induced mice, the levels of valine, leucine and isoleucine can be improved significantly in the Lvjiao Buxue Granules groups, which was a suggestion that the Lvjiao Buxue Granules could play a key role of the leukocyte elevation effect by inhibiting the BCAAs catabolism. In this study, two key enzymes, the BCKDHA and ACADS enzyme levels in a leukopenia model mice, significantly increased in the BCAAs catabolism pathway. Abnormal expression of BCAAs degrading enzymes causes BCAAs overly decomposed in leukopenia model mice. Lvjiao Buxue Granules can reverse the levels of two enzymes, thereby improving the abnormal metabolism of BCAAs.

In addition, it should be noted that whether Lvjiao Buxue Granules affects the activity of some enzymes, such as rate-limiting enzyme in the BCAAs catabolism, there is a need for further investigations. In the future, molecular biology research, isotope-labeled tracking experiments or targeted metabolomics technology could be used to further explore the biological connotation of BCAAs catabolism and their biological roles in leukopenia and the leukocyte elevation effect of Lvjiao Buxue Granules. At the same time, the key information of a biological system will be obtained with the integration of metabolites, enzymes and genes altered under a situation of leukopenia.

Conclusion

In this research, the metabolomics and the biological targets network approach were integrated to analyze and to evaluate the leukocyte elevation effects of Lvjiao Buxue Granules on mice with

cyclophosphamide-induced leucopenia. It is a demonstration that the regulation on the BCAAs catabolism pathway could play a key role in cyclophosphamide-induced leucopenia BALB/c mice after the treatment of a typical Traditional Chinese Medicine of Lvjiao Buxue Granules.

Abbreviations

BCAAs: Branched-chain amino acids; LGB: Lvjiao Buxue Granules; TCM: Traditional Chinese medicine; DST: Diyu Shengbai tablets; WBC: white blood cell count; NE: neutrophil count; LY: lymphocyte count; MO: monocytes count; RBC: red blood cell count; HGB: hemoglobin; HCT: red blood cell volume; PLT: platelet count; MCV: mean red cell volume; MCH: mean corpuscular hemoglobin; TSP: 2,2,3,3-trimethyl siliconalkyl propionate; PW: pulse width; PCA: principal component analysis; PLS-DA: partial least-squares discriminant analysis; OPLS-DA: Orthogonal-projection to latent structure-discriminant analysis; BCKDHA: branched chain keto acid dehydrogenase E1, alpha polypeptide; ACADS: Acyl-CoA Dehydrogenase Short Chain; TMAO: Trimethylamine-N-oxide; GPC: Glycerophosphocholine; PC: Phosphocholine.

Declarations

Acknowledgments

The experiments involved in this institute were completed at the Modern Research Center for Traditional Chinese Medicine, Shanxi University. The authors of this study are grateful for their supporters and funding support.

Authors' Contributions

JT, HZ and QW conceived and performed the experiments; JT and HZ wrote the paper; HZ and QW analyzed the data, HX, XX, SH and DY assisted in the execution of research; XQ design of the study and writing the protocol; All authors have understood, concurred and approved the final edition of this manuscript.

Funding

This work was financially supported by the National S&T Major Projects for “Major New Drugs Innovation and Development” (2017ZX09301047); the China Postdoctoral Science Foundation Funded Project (2016M602414).

Availability of data and materials

Data sharing is not applicable to this article as no datasets were generated or analyzed during the current study.

Consent for publication

Not applicable.

Ethics approval and consent to participate

Experiments were approved by the Ethics Committee on Animal Experiments of the Shanxi University.

Competing interests

The authors declare that they have no competing interests regarding the publication of this paper.

References

- [1] Futamura Manabu, Nagao Yasuko, Ishihara Kazuhiro, *et al.* Preoperative neoadjuvant chemotherapy using nanoparticle albumin-bound paclitaxel followed by epirubicin and cyclophosphamide for operable breast cancer: a multicenter phase II trial. *Breast Cancer-Tokyo*. 2017; 24: 615-623.
- [2] Hung CM, Hsu YC, Chen TY, *et al.* Cyclophosphamide promotes breast cancer cell migration through CXCR4 and matrix metalloproteinases. *Cell Biol Int*. 2017; 41: 345-352.
- [3] Deng J, Zhong YF, Wu YP, *et al.* Carnosine attenuates cyclophosphamide-induced bone marrow suppression by reducing oxidative DNA damage. *Redox Biol*. 2017; 14: 1-6.
- [4] Sun X, Zhao YN, Qian S, *et al.* Ginseng-derived panaxadiol saponins promote hematopoiesis recovery in cyclophosphamide-induced myelosuppressive mice: Potential novel treatment of chemotherapy-induced cytopenias. *Chin J Intergr Med*. 2018; 3: 1-7.
- [5] Mellor D, Prieto E, Mathieson L, *et al.* A Kernelisation Approach for Multiple d-Hitting Set and Its Application in Optimal Multi-Drug Therapeutic Combinations. *PloS One*. 2010; 5: e13055.
- [6] Gu JF, Feng L, Zhang MH, *et al.* New exploration on effect of characteristics of traditional Chinese medicine components structure on multi-ingredient/component pharmacokinetics. *Chin J Chin Mater Med*. 2014; 39: 2782-2786.
- [7] Liu CC, Liu H, Gu ZX, *et al.* Mechanisms of tonifying blood with Lvjiao Buxue Granules studied by ¹H-NMR metabolomics. *Chinese Traditional and Herbal Drugs*. 2016; 47: 1142-1148.
- [8] An MP, Zhang SY, Zhang Y, *et al.* Effect of Asini Corii Colla on immune function in hypimmune mice. *Drug Eval Res*. 2018; 41: 567-571.

9. [9] Zhang W, Zhu JH, Xu H, *et al.* Five Active Components Compatibility of Astragali Radix and Angelicae Sinensis Radix Protect Hematopoietic Function Against Cyclophosphamide-Induced Injury in Mice and t-BHP-Induced Injury in HSCs. *Front Pharmacol.* 2019; 10: 936-951.
10. [10] Huang YY, Zhang Y, Kang LP, *et al.* Research progress on chemical constituents and their pharmacological activities of plant from Codonopsis. *Chinese Traditional and Herbal Drugs.* 2018; 49: 239-250.
11. [11] Tang BB, Zhou DH, He XM, *et al.* Study on Medication Rule of TCM Compound Prescription in Treatment of Leukopenia after Radiotherapy and Chemotherapy for Malignant Tumor. *Acta Chinese Medicine.* 2018; 33: 1838-1842.
12. [12] Hu QD, Wu WH, Zeng Y, *et al.* Blood metabolism study on protection of residual renal function of hemodialysis patients by traditional Chinese medicine Kidney Flaccidity Compound. *Cell Mol Biol.* 2018; 64: 107-112.
13. [13] Sun H, Li XN, Zhang AH, *et al.* Exploring potential biomarkers of coronary heart disease treated by Jing Zhi Guan Xin Pian using high-throughput metabolomics. *RSC Adv.* 2019; 9: 11420-11432.
14. [14] Wang WB, Zhao LL, He ZY, *et al.* Metabolomics-based evidence of the hypoglycemic effect of Ge-Gen-Jiao-Tai-Wan in type 2 diabetic rats via UHPLC-QTOF/MS analysis. *J Ethnopharmacol.* 2018; 219: 299-318.
15. [15] Tian JS, Meng Y, Wu YF, *et al.* A novel insight into the underlying mechanism of Baihe Dihuang Tang improving the state of psychological suboptimal health subjects obtained from plasma metabolic profiles and network analysis. *J Pharmaceut Biomed.* 2019; 169: 99-110.
16. [16] Tian JS, Peng GJ, Wu YF, *et al.* A GC-MS urinary quantitative metabolomics analysis in depressed patients treated with TCM formula of Xiaoyaosan. *J Chromatogr B.* 2016; 1026: 227-235.
17. [17] Qu TL, Wang EB, Li AP, *et al.* NMR based metabolomic approach revealed cyclophosphamide-induced systematic alterations in a rat model. *RSC Adv.* 2016; 6: 111020-111030.
18. [18] Huyan XH, Lin YP, Gao T, *et al.* Immunosuppressive effect of cyclophosphamide on white blood cells and lymphocyte subpopulations from peripheral blood of BALB/c mice. *Int Immunopharmacol.* 2011; 11: 1293-1297.
19. [19] Fan C, Georgiou KR, Morris HA, *et al.* Combination breast cancer chemotherapy with doxorubicin and cyclophosphamide damages bone and bone marrow in a female rat model. *Breast Cancer Res Tr.* 2017; 165: 1-11.
20. [20] Luo GF, Tang YH, Wu LF, *et al.* Haematology, Protective effects of Qianggushengxue oral liquid on chemotherapy-induced bone marrow suppression in mice. *Chinese Journal of New Drugs.* 2017; 26: 2664-2671.
21. [21] Huang JQ, Pang MR, Li GY, *et al.* Alleviation of cyclophosphamide-induced immunosuppression in mice by naturally acetylated hemicellulose from bamboo shavings. *Food Agr Immunol.* 2017; 28: 328-342.
22. [22] Khan MA. Immune potentiating and antitoxic effects of camel milk against cyclophosphamide-induced toxicity in BALB/c mice. *Int J Health Sci.* 2017; 11: 18-22.

23. [23] Zhang L, Gong Amy GW, Riaz K, *et al.* A novel combination of four flavonoids derived from Astragali Radix relieves the symptoms of cyclophosphamide-induced anemic rats. *FEBS Open Bio.* 2017; 7: 318-323.
24. [24] Christen D, Brümmendorf TH, Panse J. Leukopenia - A Diagnostic Guideline for the Clinical Routine. *Dtsch Med Wochenschr.* 2017; 142: 1744-1749.
25. [25] Cook ES, Nutini LG. Counteraction of leukopenia caused by mechlorethamine and azathioprine. *J Surg Oncol.* 1971; 3: 131-141.
26. [26] Stroda KA, Murphy JD, Hansen RJ, *et al.* Pharmacokinetics of cyclophosphamide and 4-hydroxycyclophosphamide in cats after oral, intravenous, and intraperitoneal administration of cyclophosphamide. *Am J Vet Res.* 2017; 78: 862-866.
27. [27] Zhang XL, Lu YS, Jian JC, *et al.* Cloning and expression analysis of recombination activating genes (RAG1/2) in red snapper (*Lutjanus sanguineus*). *Fish Shellfish Immun.* 2012; 32: 534-543.
28. [28] Duan XX, Gao S, Li JL, *et al.* Acute arsenic exposure induces inflammatory responses and CD4⁺ T cell subpopulations differentiation in spleen and thymus with the involvement of MAPK, NF- κ B, and Nrf2. *Mol Immunol.* 2017; 81: 160-172.
29. [29] Mahaki H, Jabarivasal N, Sardarian K, *et al.* The effects of extremely low-frequency electromagnetic fields on c-Maf, STAT6, and ROR α expressions in spleen and thymus of rat. *Electromagn. Biol Med.* 2019; 38: 1-7.
30. [30] Sasaguri K, Yamada K, Narimatsu Y, *et al.* Stress-induced galectin-1 influences immune tolerance in the spleen and thymus by modulating CD45 immunoreactive lymphocytes. *J Physiol Sci.* 2017; 67: 489-496.
31. [31] Yang L, Yan CY, Zhang F, *et al.* Effects of ketoconazole on cyclophosphamide metabolism: evaluation of CYP3A4 inhibition effect using the in vitro and in vivo models. *Exp Anim.* 2018; 67: 71-82.
32. [32] Lin ST, Hao GX, Long M, *et al.* Oyster (*Ostrea plicatula* Gmelin) polysaccharides intervention ameliorates cyclophosphamide-Induced genotoxicity and hepatotoxicity in mice via the Nrf2-ARE pathway. *Biomed Pharmacother.* 2017; 95: 1067-1071.
33. [33] Olayinka ET, Ore A, Ola OS, *et al.* Ameliorative Effect of Gallic Acid on Cyclophosphamide-Induced Oxidative Injury and Hepatic Dysfunction in Rats. *Medical Sciences.* 2015; 3: 78-92.
34. [34] Stankiewicz A, Skrzydlewska E. Protection against cyclophosphamide-induced renal oxidative stress by amifostine: the role of antioxidative mechanisms. *Toxicolo Mech Method.* 2003; 13: 301-308.
35. [35] Holeček M. Branched-chain amino acids in health and disease: metabolism, alterations in blood plasma, and as supplements. *Nutr Metab.* 2018; 15: 33.
36. [36] Yamada T, Matsuzaki M, Tanaka A. Increase in insulin secretion and decrease in muscle degradation by fat-free milk intake are attenuated by physical exercise. *Clin Chim Acta.* 2018; 484: 21-25.

37. [37] Ikeda T, Ikeda T, Jinno T, *et al.* Effect of exercise therapy combined with branched-chain amino acid supplementation on muscle strengthening in persons with osteoarthritis. *Hong Kong Physiother J.* 2018; 38: 23-31.
38. [38] Xu MJ, Kitaura Y, Shindo D, *et al.* Branched-chain amino acid (BCAA) supplementation enhances adaptability to exercise training of mice with a muscle-specific defect in the control of BCAA catabolism. *Biosci Biotech Bioch.* 2018; 82: 1-4.
39. [39] Lashinger LM, Rasmussen AJ, Malone L, *et al.* Abstract 809: dietary l-leucine diminishes protective effects of calorie restriction in a transplant model of pancreatic cancer. *Cancer Research*, 71(8 Supplement), 809-809. Abstract 809: Dietary L-Leucine diminishes protective effects of calorie restriction in a transplant model of pancreatic cancer. *Cancer Res.* 2011; 71: 809.
40. [40] Gatti R, Cappellin E, Schiraldi C, *et al.* Plasma lactate, GH and GH-binding protein levels in exercise following BCAA supplementation in athletes. *Amino Acids.* 2001; 20: 1-11.
41. [41] Liu MH, Li PL, Zeng X, *et al.* Identification and pharmacokinetics of multiple potential bioactive constituents after oral administration of radix astragali on cyclophosphamide-induced immunosuppression in BALB/c mice. *Int J Mol Sci.* 2015; 16: 5047-5071.
42. [42] Búfalo MC, Sforcin JM. The modulatory effects of caffeic acid on human monocytes and its involvement in propolis action. *J Pharm Pharmacol.* 2015; 67: 740-745.

Figures

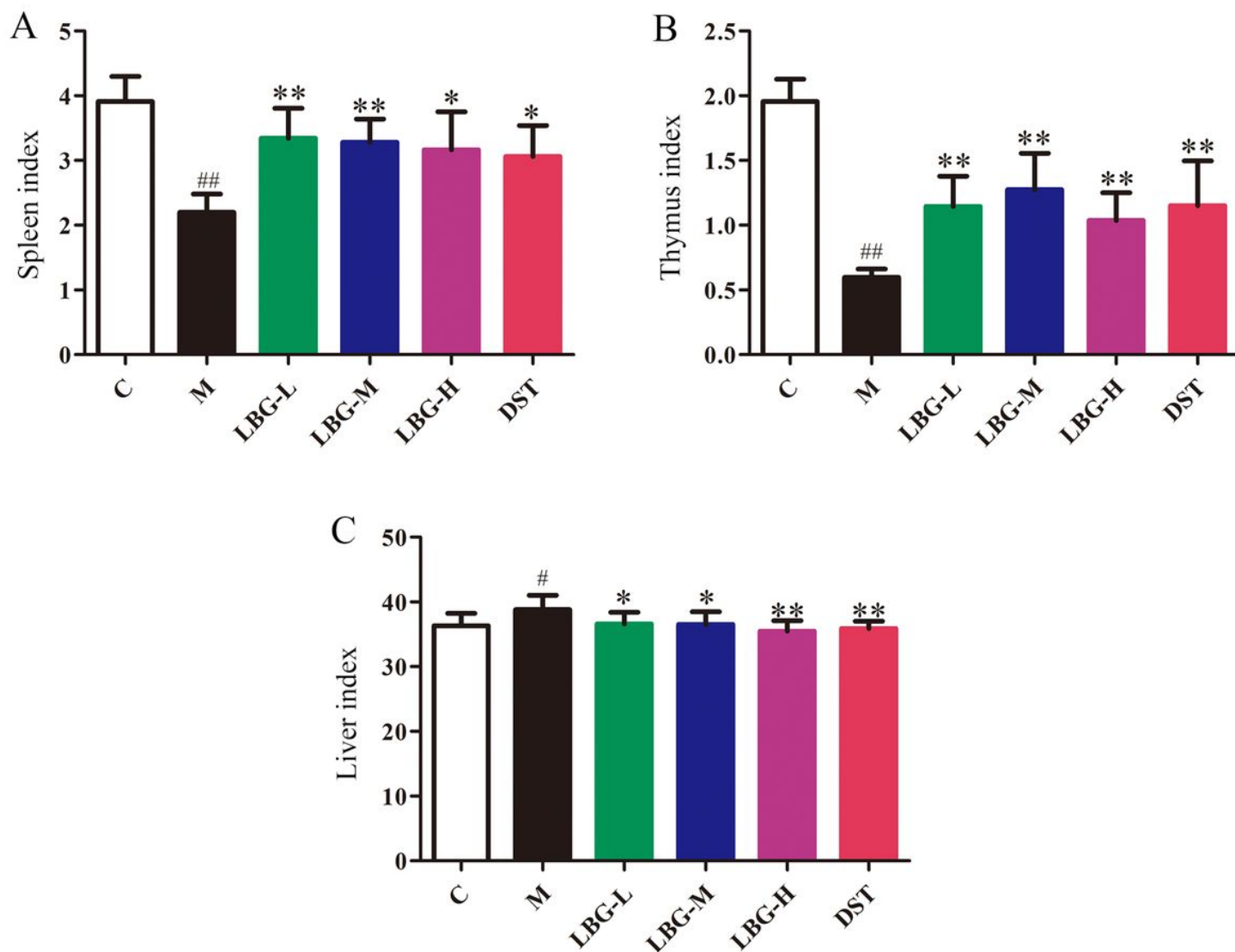


Figure 1

The effects of LBG on organ indexes (n=8). (A) Spleen index. (B) Thymus index. (C) Liver index. Data are expressed as mean \pm S.D. #P < 0.01 vs. C group; ##P < 0.01 vs. C group; *P < 0.05 vs. M group; **P < 0.01 vs. M group.

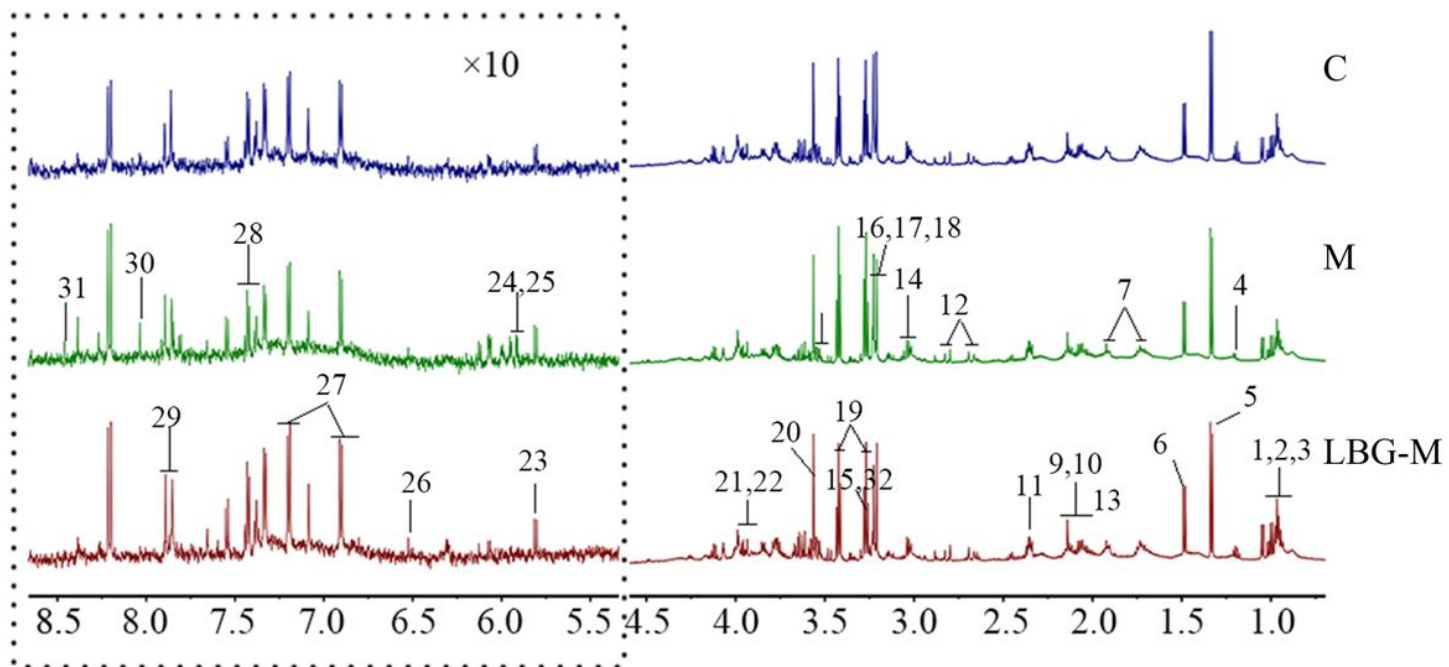


Figure 2

The ^1H NMR spectra of mice spleen tissue in C, M and LBG-M groups.

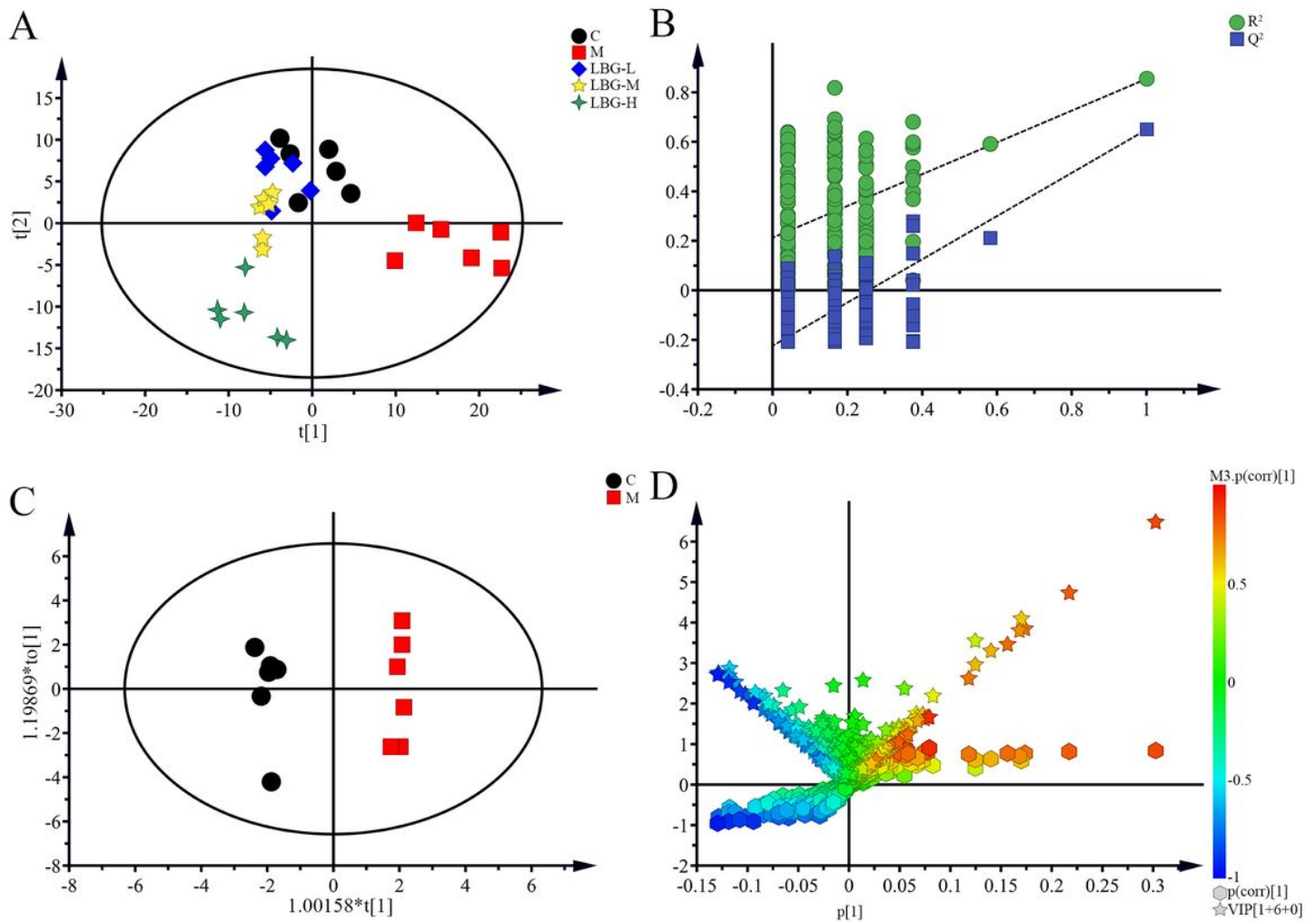


Figure 3

Pattern recognition of Simca-P14.1. (A) Results of multiple pattern recognition of spleen metabolites in C, M, LBG groups. PLS-DA score plot (n=6). (B) Results of permutation tests. $R^2=0.854$, $Q^2=0.649$. (C) OPLS score plot (n=6, $R^2Y=0.947$, $R^2X=0.431$, $Q^2=0.659$) of C group and M group. (D) OPLS (S+V)-plot of C group and M group. Each point in the (S+V)-plot represents an ion. Ions far away from the origin were potential biomarkers.

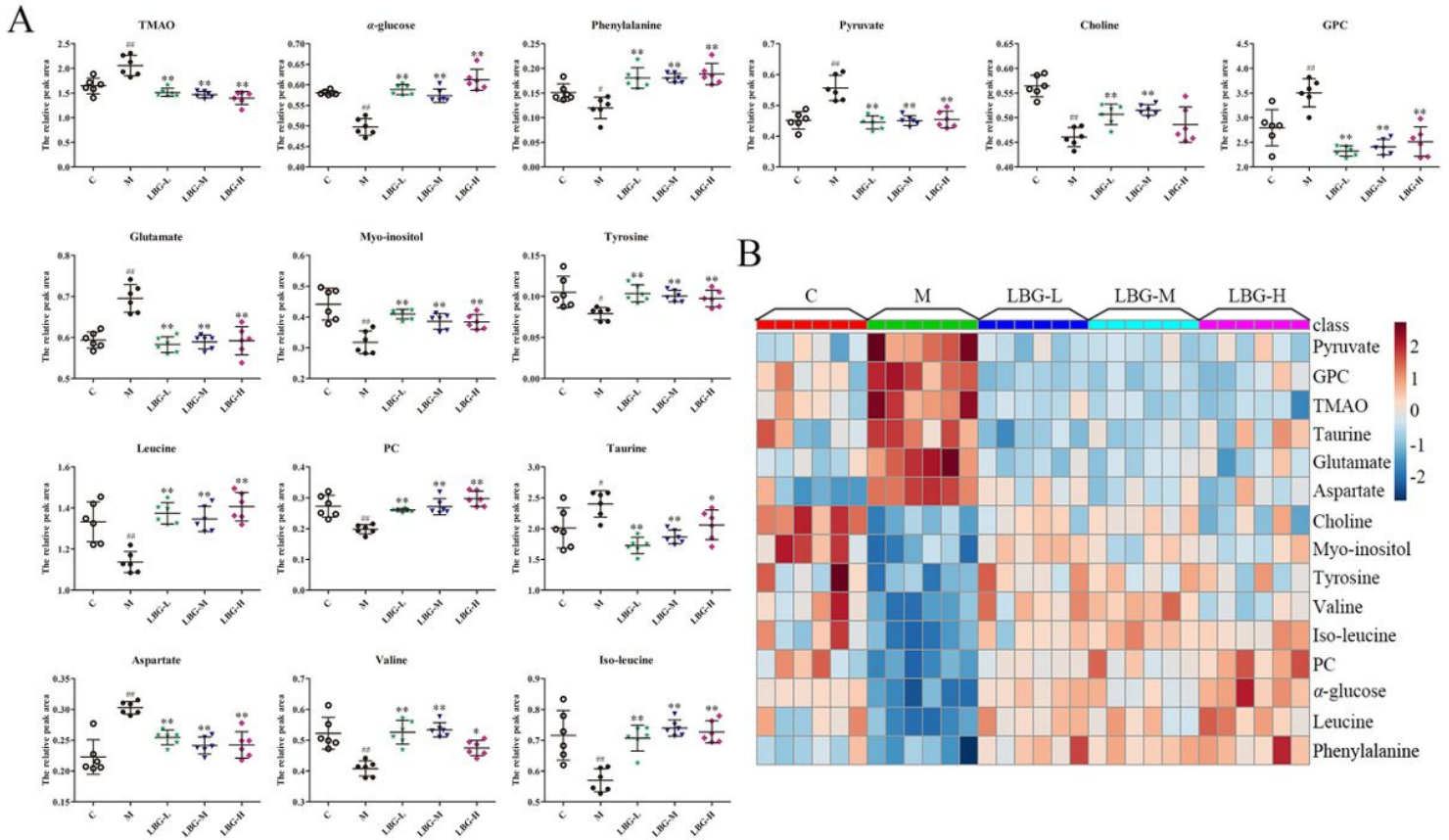


Figure 4

(A) Box-plots of the changes of differential metabolites of mice spleens in C, M and LBG groups. Data are expressed as mean \pm S.D. #P < 0.05 vs. C group; ##P < 0.01 vs. C group; *P < 0.05 vs. M group; **P < 0.01 vs. M group. (B) The relative content of the heatmap of differential metabolites in mice spleens. The ribbon -3~3: represents the relative content of the differential metabolites from low to high.

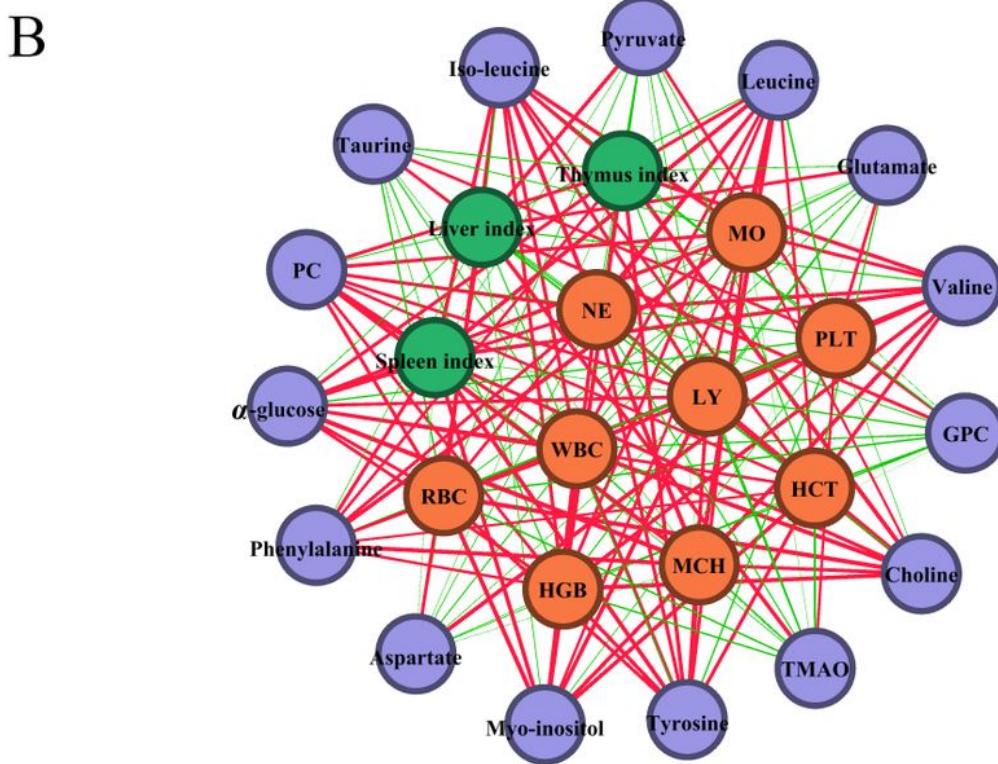
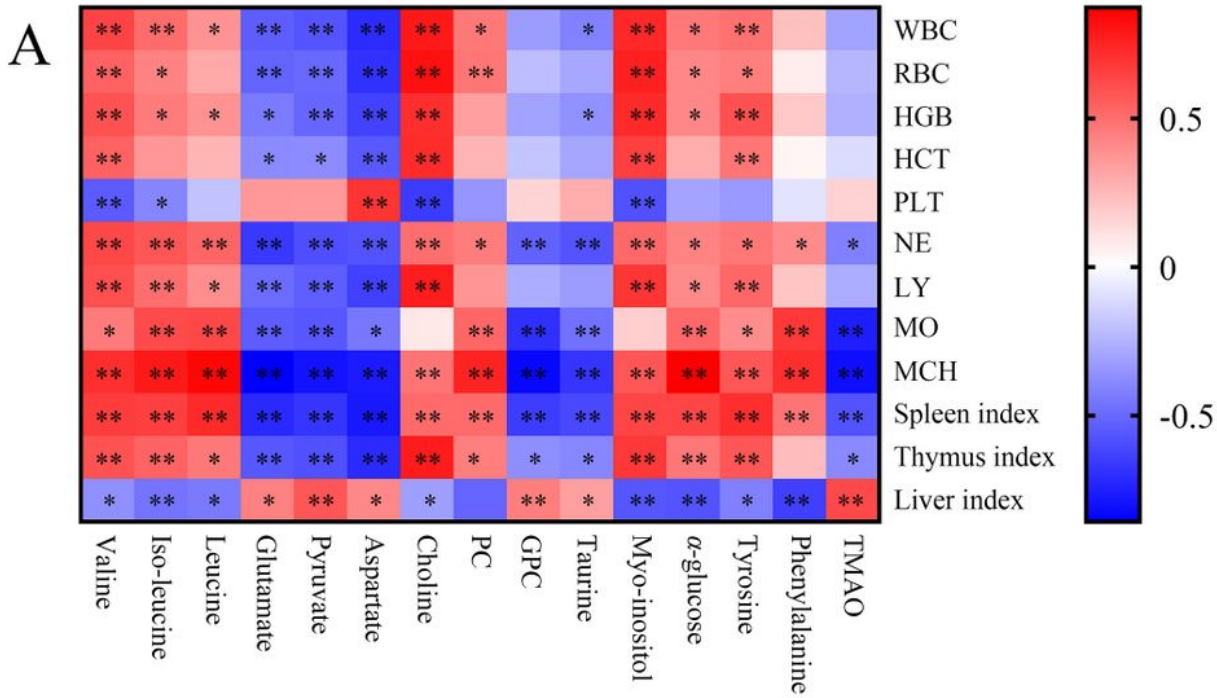


Figure 5

Correlation analysis of differential metabolites, blood routine parameters and organ indexes. (A) The correlation map of differential metabolites, blood routine parameters and organ indexes. Red and blue represent positive and negative correlations respectively (* $P < 0.05$, ** $P < 0.01$). (B) Correlation network of differential metabolites, blood routine parameters and organ indexes based on Pearson's correlation coefficients. Purple, yellow and green node represent differential metabolites, blood routine parameters

and organ indexes. Red and green line represent positive and negative correlations. Line thickness reflects the magnitude of the correlation coefficients.

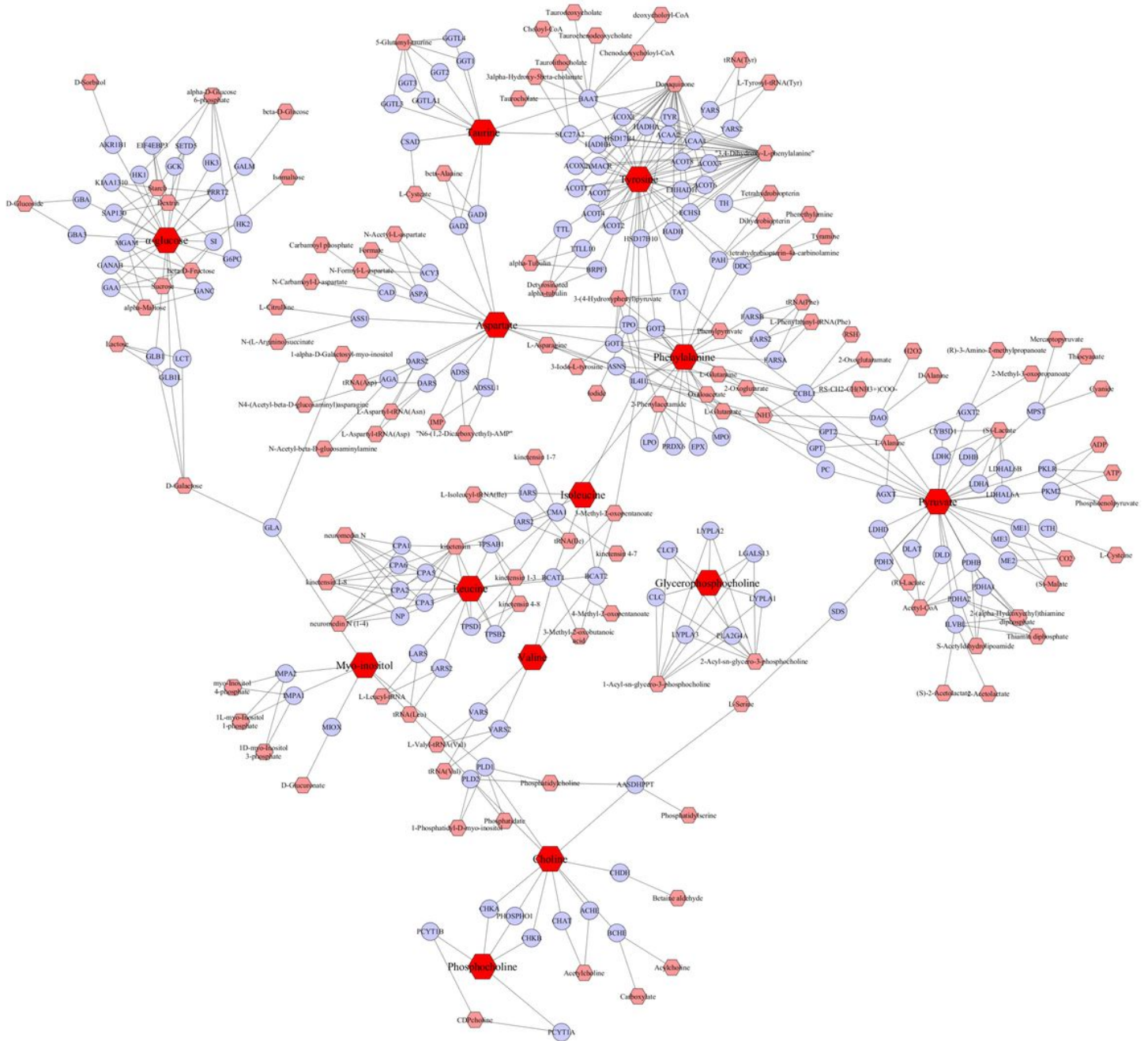


Figure 6

The metabolic networks involved in enzymes, genes and related-compound were established based on the differential metabolites. Red, light-blue and pink node represent differential metabolites, enzymes/genes and related-compound.

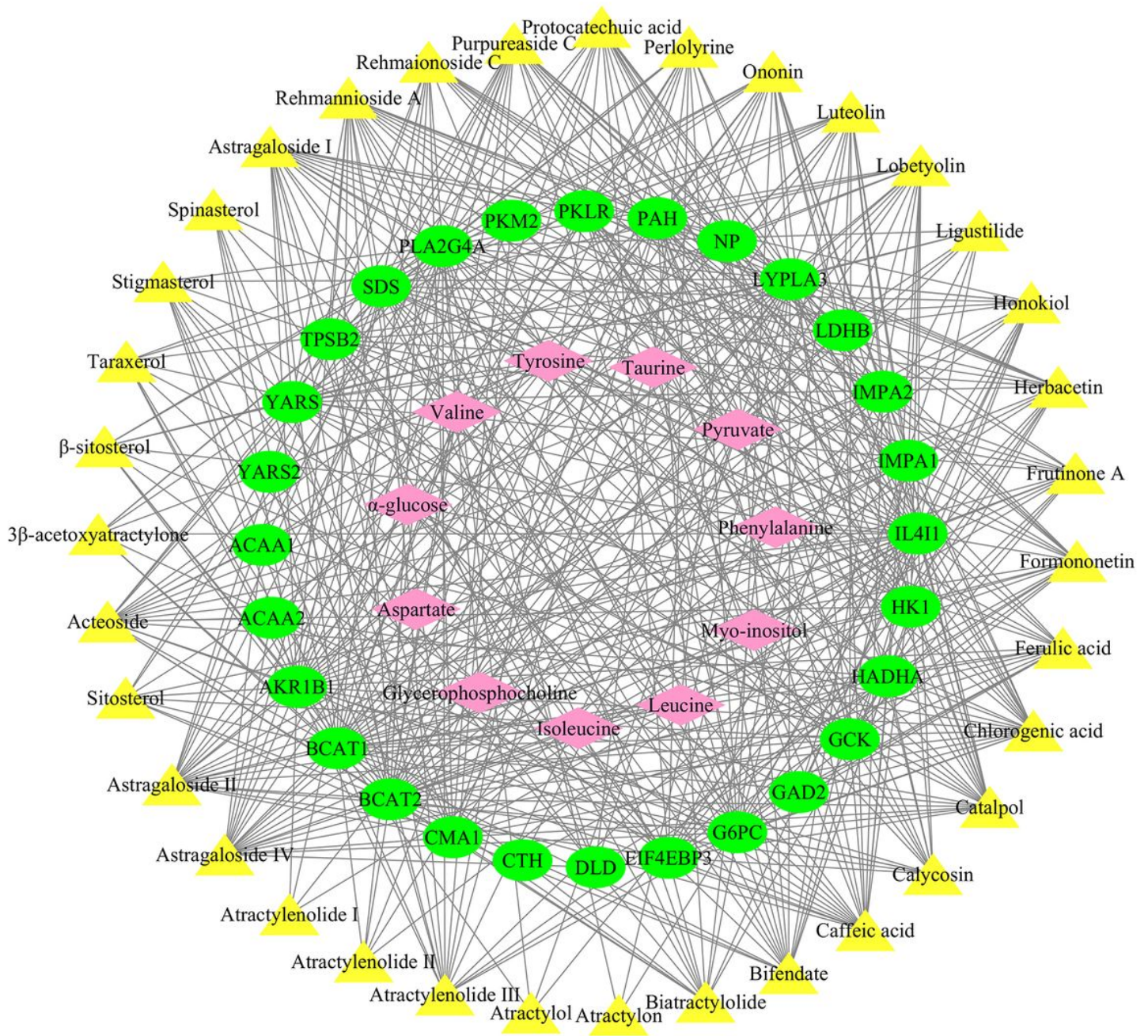


Figure 7

“chemical components-targets-differential metabolites” regulatory network of LBG. Yellow nodes represent the chemical components, green nodes represent the targets, and pink node represent differential metabolites.

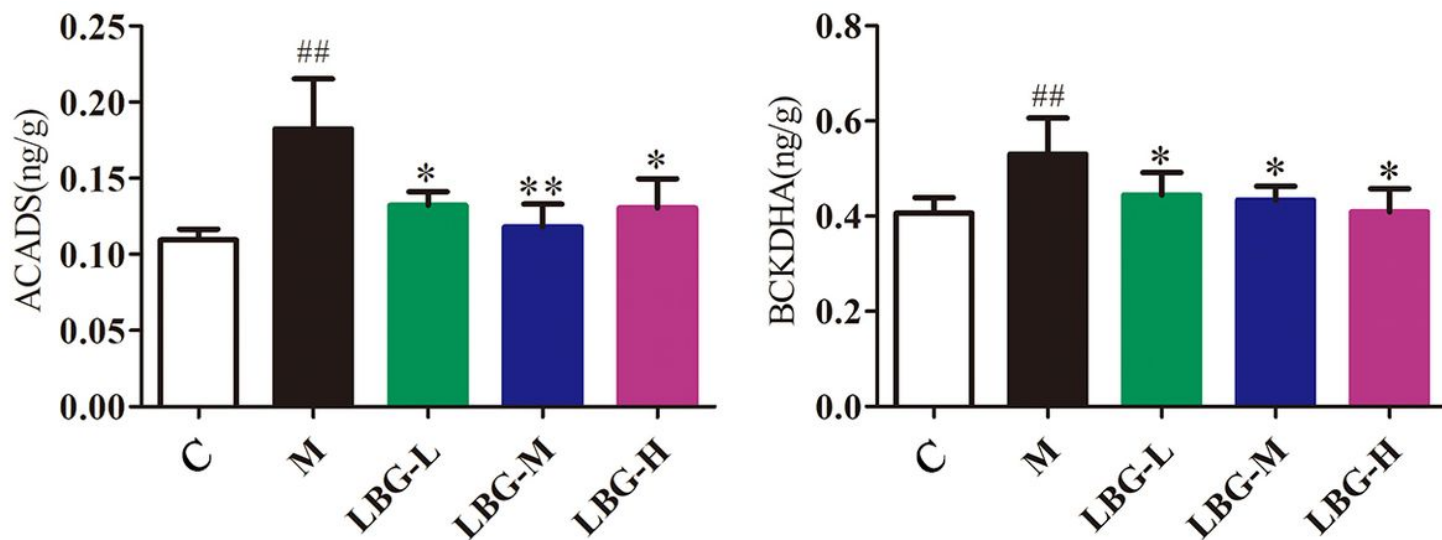


Figure 8

Expression of ACADS and BCKDHA enzyme levels in mice liver tissue using ELISA analysis. Data are expressed as mean \pm S.D. ##P < 0.01 vs. C group; *P < 0.05 vs. M group; **P < 0.01 vs. M group.

VALINE, LEUCINE AND ISOLEUCINE DEGRADATION

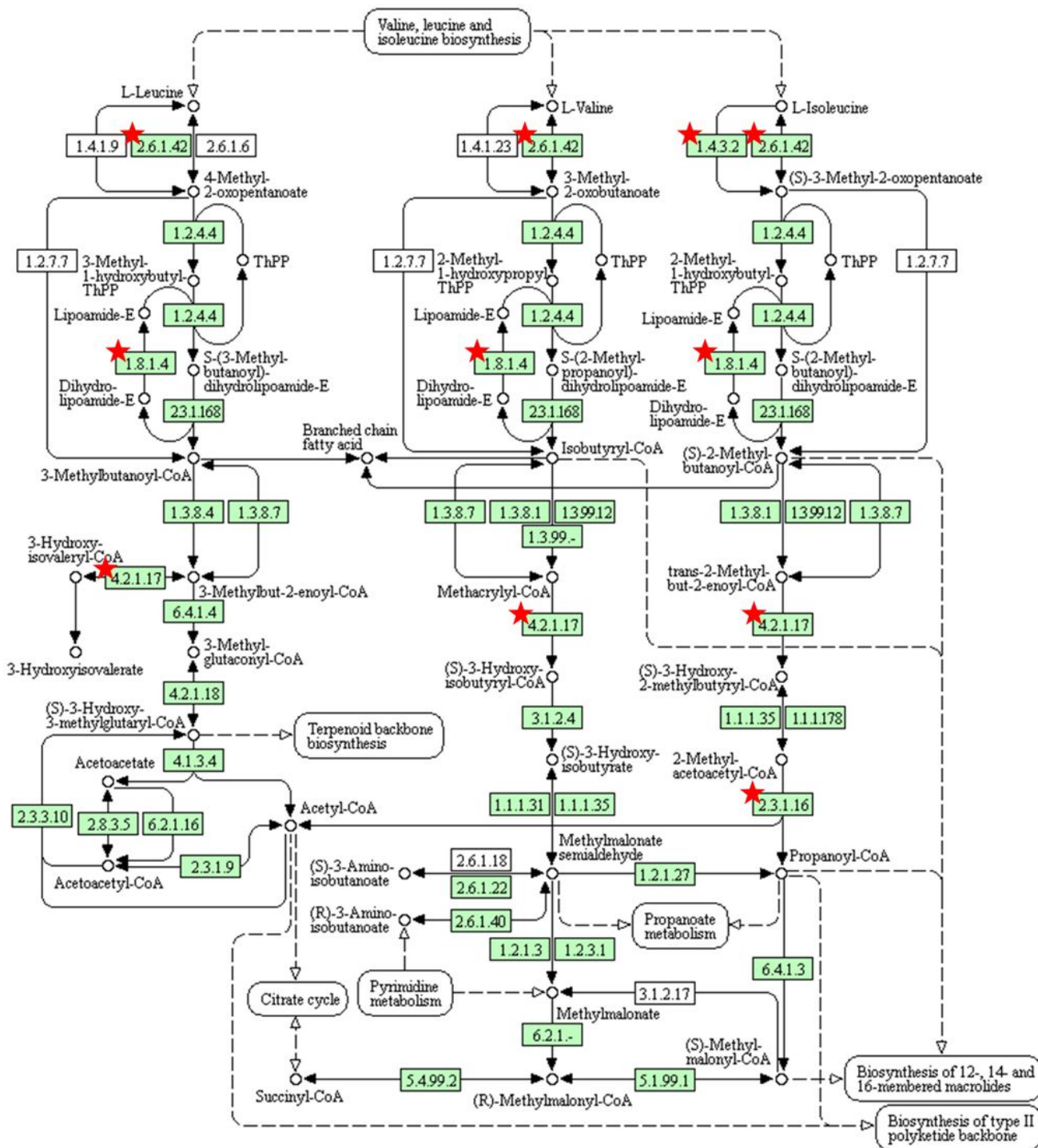


Figure 9

Pathway of branched chain amino acids catabolism found by KEGG Pathway Maps. The organism-specific pathways are colored green, where coloring indicates that map objects exist and are linked to corresponding entries. The red stars mark potential targets of LBG in pathways. It is indicated that Lvjiao Buxue Granules attenuates cyclophosphamide-Induced leucopenia by regulating branched chain amino acids catabolism pathway.

Supplementary Files

This is a list of supplementary files associated with this preprint. Click to download.

- [SupplementMaterial.doc](#)
- [GraphicalAbstract.tif](#)